WFILAS: WIDE FIELD IMAGER LYMAN ALPHA SEARCH

EDUARD WESTRA[1], D. Heath Jones[1], Chris Lidman[2], Ramana Athreya[3], Klaus Meisenheimer[4],
Christian Wolf[5], Thomas Szeifert[2], Emanuela Pompei[2], Leonardo Vanzi[2]

[1] *Mt. Stromlo Observatory, Research School of Astronomy & Astrophysics, Australia*
[2] *European Southern Observatory, Chile*
[3] *National Centre for Radio Astrophysics, India*
[4] *Max Planck Institute für Astronomie, Germany*
[5] *Department of Physics, University of Oxford, United Kingdom*

Abstract. The Wide Field Imager Lyman-Alpha Search (WFILAS) is a search for Lyα emitting galaxies at $z \sim 5.7$. Deep images from the Wide Field Imager (WFI) on the ESO/MPI 2.2 m telescope have been used to detect 7 bright Lyα emitting candidates in three fields covering 0.74 sq. degree on the sky. For this we used three narrowband (FWHM ~ 70 Å), one encompassing intermediate band (FWHM ~ 220Å) and broadband B and R filters. One has thus far been spectroscopically confirmed as a Lyα emitting galaxy at $z = 5.721$ using FORS2 at the VLT. This galaxy shows a bright, well resolved asymmetric line profile, which is characteristic of Lyα emitting galaxies.

In one of our three fields, the Chandra Deep Field South (CDFS), we find an overdensity of Lyα emitters in agreement with other surveys that have targeted this region. A statistically complete sample of our candidates probes the bright-end of the luminosity function, confirming earlier results from other smaller, deeper surveys.

1 Introduction

To be able to derive the star formation history of the Universe, it is necessary to determine the star formation rate at several redshifts. Emission lines are good probes for this, as the star formation rate is proportional to the line luminosity. The hydrogen Balmer series is particularly well suited for this purpose. The Balmer emission line luminosity is directly proportional to the total ionising flux of the young OB stars embedded in H II regions, which is equatable to the rate at which they form [8]. Other lines, such as [O II] and [O III], can be used as well, although the metallicity of the surrounding gas needs to be taken into account. In all cases, the line luminosities need to be corrected for internal extinction due to dust. ([8]; and references therein). It is also possible to use Lyα as star formation indicator, though extinction corrections are much higher, because the line is in the rest-frame ultraviolet. By using narrowband filter surveys it is possible to probe several of these emission lines at different redshifts.

2 WFILAS

The Wide Field Imager Lyman Alpha Search (WFILAS) is a narrowband filter survey designed to detect Lyα emitting galaxies at $z \sim 5.7$. It was undertaken with the 2.2 m ESO/MPI telescope at Cerro La Silla with the Wide Field Imager (WFI). We targeted three fields to be able to assess the influence of cosmic variance. The fields are the Chandra Deep Field South (CDFS), a field near the South Galactic Pole (SGP) and the COMBO-17 S11 field. This yields a total sky coverage of 0.74 sq. degree, which gives a volume of 1.0×10^6 Mpc^3 at $z \sim 5.7$[1]. Together with the relatively bright survey limit ($m_{AB} \sim 24.0-24.5$) we expect to find Lyα emitting galaxies at the bright end of the luminosity function.

This survey is unique in its filter setup. Instead of the usual single narrowband filters we have used three neighbouring narrowband filters encompassed by one intermediate band filter (FWHM ~ 220 Å). The particular narrow bandpass (FWHM ~ 70 Å) of the narrowband filters provides a high contrast for line emitting galaxies. This is demonstrated in Figure 1. Two examples are given, a low redshift galaxy (spectrally confirmed to be an Hα emitting galaxy at $z = 0.25$) and a candidate high redshift galaxy (still to be confirmed). In both cases the galaxy is visible in the narrowband image in which emission line resides, particulary in the low redshift case.

Using the images that were taken in the broadband B and R filters[2], we are able to minimise the contamination of low redshift line emitting galaxies, as Lyα galaxies have no continuum bluewards of the Lyα line. At the same time, we can use these low redshift candidates to measure the star formation rate at their respective

---

[1] Throughout this paper we assume $H_0 = 70$ km s^{-1} Mpc^{-1}, $\Omega_M = 0.3$ and $\Omega_\Lambda = 0.7$
[2] The broadband B and R and a fraction of the intermediate band M_{815} data have been taken from the COMBO-17 survey [13]

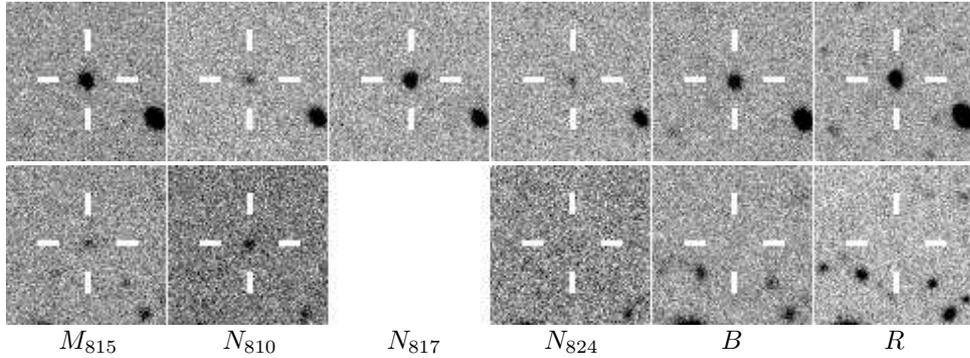| M_{815} | N_{810} | N_{817} | N_{824} | B | R |

Figure 1: Two examples of candidate line emitting galaxies. These figures demonstrate the contrast of the narrowband filters and the use of the broadband B and R data to distinguish between low and high redshift galaxies. From left to right are the intermediate band filter M_{815}, three narrowband filters N_{810}, N_{817} and N_{824}, and the broadband filters B and R. (*top*) Line emitting galaxy confirmed to be at $z = 0.25$. The galaxy is clearly visible in N_{817}. The strong Hα line of this galaxy resides in the spectral range of this filter. In the neighbouring N_{810} and N_{824} filter the continuum of the galaxy can be seen. Furthermore, this galaxy is visible in both broadband filters, which confirm the low redshift nature of the galaxy. (*bottom*) Candidate $z \sim 5.7$ line emitting galaxy. In this case the possible Lyα line resides in the spectral range of the N_{810} filter. There is no N_{817} available for the second object. Moreover, there is no detection in both broadband filters, strengthening the case of the line being Lyα. If confirmed, this galaxy will have the strongest Lyα line at this redshift ($\sim 1 \times 10^{-16}\,\mathrm{erg\,s^{-1}\,cm^{-2}}$).

redshifts. We will touch on this aspect of the survey in Section 5 in combination with the Taurus Tuneable Filter Field Galaxy Survey.

3 Confirmed Lyα Emitter at $z = 5.721$

One of the candidate Lyα emitting galaxies (see Figure 2 for the thumbnails) has been confirmed with follow-up spectroscopy [12]. The object shows a strong detection in only one of the narrowband images, N_{817}, and also in the intermediate band image, M_{815}. In both B and R there is no detection at the location of the object. In March 2004 the object J114334.98−014433.9 was observed with VLT/FORS2 at medium resolution (R $\sim$ 3600). In the spectrum only one emission line is visible (see Figure 2). This line is clearly asymmetric, which is a strong indication for Lyα [10]. Additionally, the lack of any other emission lines in our spectrum, such as Hβ, [O II], or [O III], support that the line is Lyα and not an emission line at lower redshift, e.g. Hα at $z \sim 0.24$. The line is not [O II] $\lambda\lambda3726,3728$, because the resolution of the spectrum is high enough to resolve the doublet. Based on these arguments, we conclude that the emission line is Lyα.

From the spectrum we derived a line flux of $5 \times 10^{-17}\,\mathrm{erg\,s^{-1}\,cm^{-2}}$, making it one of the brightest Lyα emitters at this redshift (cf. [2, 6]). This translates to a line luminosity of $1.8 \times 10^{43}\,\mathrm{erg\,s^{-1}}$, which is in accordance with the original survey goals of large volume and bright survey limit.

We fitted the emission line in a similar fashion as [6] with a truncated Gaussian (see Figure 2b,c). If we add a second, narrower and weaker Gaussian to the model, we are able to fit the second peak in the red wing of the line much better. Fitting in this way gave us two solutions, both with the second peak at $\sim$400 km s^{-1} redshifted from the truncated Gaussian profile, but one being broader and less strong than the other. We are unable to distinguish between the two models given their similar χ^2_ν. In general, a second peak in the Lyα line is a clear signature of an expanding shell of neutral hydrogen [1, 4].

4 Results of WFILAS

WFILAS has yielded 7 candidate Lyα emitting galaxies at $z \sim 5.7$ in the range of $1-3 \times 10^{43}\,\mathrm{erg\,s^{-1}}$, corresponding[3] to $\sim 10-30\,\mathrm{M_\odot\,yr^{-1}}$. One of these is the confirmed Lyα emitter at $z \sim 5.721$ (Section 3). The remaining candidates await spectral confirmation.

We have defined two samples: the *entire* sample and a *statistically complete* sample. The entire sample contains all the candidates. The statistically complete sample contains the candidates from our four deepest narrowband images. The candidates in the complete sample are also above a flux limit, which is set at $M_{\mathrm{AB}} = 23.38$. Finally, we corrected the sample for completeness. In Figure 3 we have combined our completeness-corrected

---

[3]To convert between luminosity and star formation rate, we use the conversion rate SFR(Lyα) $= 9.1 \times 10^{-43}\,\mathrm{L(Ly\alpha)\,M_\odot\,yr^{-1}}$, from [2]
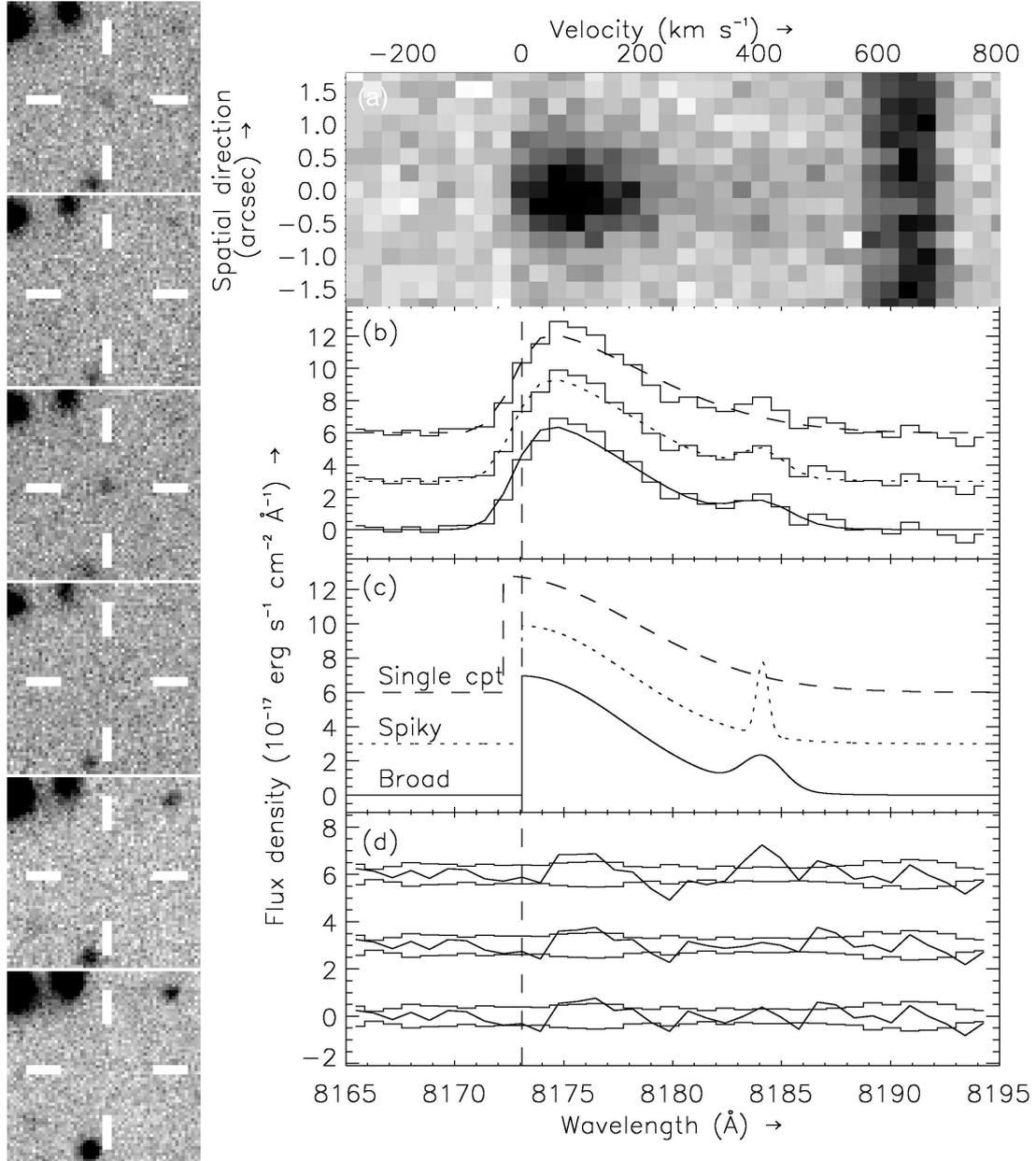
Figure 2: (*left*) Thumbnail images of the confirmed Lyα galaxy J114334.98−014433.9 in different filters, from top to bottom: intermediate band filter M_{815}, narrowband filters N_{810}, N_{817}, N_{824} and broadband filters B and R. (*right*) A fit of the Lyα line with one- and two-component models. (*a*) The two dimensional spectrum centered on the Lyα line. In this unrectified spectrum, the night sky emission lines have not been removed. The pixel scale is $0\farcs252\,\mathrm{pix}^{-1}$ in the spatial direction and $0.86\,\mathrm{\AA\,pix}^{-1}$ in the dispersion direction. (*b*) Observed Lyα line (*histograms*) with the three best-fitting models. For clarity, the models are offset by $3 \times 10^{-17}\,\mathrm{erg\,s}^{-1}\,\mathrm{cm}^{-2}\,\mathrm{\AA}^{-1}$. The two-component models consist of a broad, truncated Gaussian and a narrower redshifted Gaussian. The one-component model consists of only a broad, truncated Gaussian. (*c*) Same model line profiles as in (*b*) but before convolution with the instrument profile. (*d*) Observed data minus model fit (as plotted in (*b*)) residuals, demonstrating a random scatter about the zero flux line. Also shown (*histograms*) is the 1σ-error spectrum from the observed data, which includes poissonian noise from both the sky and the object. Note that the red peak is not the N v line. At this redshift it would appear around $8334\,\mathrm{\AA}$.

sample with a completeness-corrected sample from Ajiki [2]. Also shown are two Schechter function fits: one for the Ajiki sample alone, without the lowest two luminosity bins and a fit for the combined sample of WFILAS and Ajiki (without the lowest two luminosity bins). For both fits we assumed a slope of $\alpha = -1.53$, which [2] adopted from the Hα luminosity function at $z \sim 0.24$ from [5], since neither sample goes deep enough to constrain this part of the luminosity function. It can be seen that the WFILAS sample complements other surveys, which do not cover a volume as large as that covered by WFILAS.
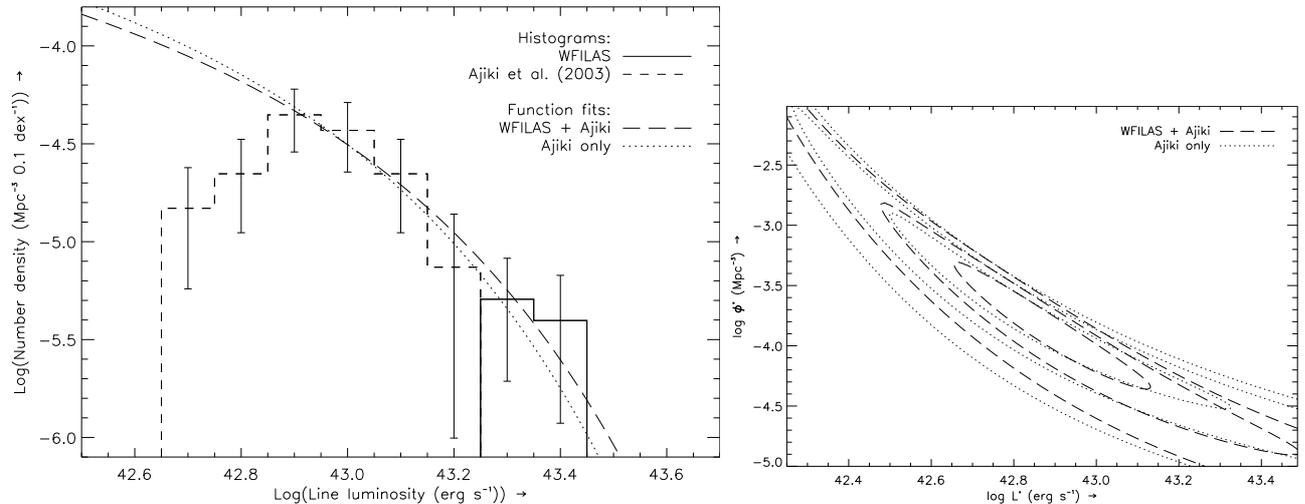

Figure 3: Line luminosity distribution of the complete sample of Lyα candidates (*solid histogram*) together with the candidates from [2] (*dashed histogram*) are plotted in the left figure. Both samples are corrected for completeness. The errorbars are derived using Poisson statistics. Furthermore, two Schechter function fits are indicated: one for the combined WFILAS and Ajiki sample (*dotted*) and one for the Ajiki sample alone (*long dashed*). The right figure shows the 68.3%, 95.4% and 99.7% confidence limits for the fitting parameters L^* and ϕ^*. As there is little data at faint luminosities, phi^* and L^* are highly correlated.

We note that the number of Lyα emitting galaxies in the two faintest bins is considerably less than that predicteed by the fitted luminosity function. If this is not incompleteness, then the reason for the drop in the number density of faint sources needs to be understood. It might be related to the star formation rate. If the rate is too low, the associated H II region will be too small and most Lyα photons might be unable to escape the slowly expanding envelope of neutral hydrogen that surrounds the H II region.

Another result from the WFILAS survey is that in one of the fields we find an overdensity of sources in the south-eastern part of our fields, the CDFS (see Figure 4). To enhance this result, we have added to our candidates the i'-dropout of [3] at $z = 5.78$, which is located in the same area of the field. This overdensity is entirely in agreement with the results of [11] and the recent discovery of an overdensity at a similar redshift in the Hubble Ultra Deep Field, which is enclosed in our field. This result demonstrates the importance of having a wide field of view not only to find the bright end of the luminosity function, but also to elucidate variations in large scale structures.

5   Taurus Tuneable Filter Field Galaxy Survey

One of the advantages of WFILAS is that it is also suitable to pick up low redshift galaxies (see Section 2 and Figure 1). In addition to this, we will use follow-up spectroscopy to the Taurus Tuneable Filter Field Galaxy Survey (TTFFGS; [7]). The TTFFGS is a survey designed to find low redshift emission line galaxies, such as Hα, Hβ, [O II] and [O III]. For the survey we used the (now decommissioned) Taurus Tuneable Filter at the Anglo-Australian Telescope. The filter is a Fabry-Perot interferometer able to create very narrow filter passbands (FWHM $\sim 20-30$Å) with an Airy profile at a user-specified central wavelength. An order-sorting filter is necessary to remove other passbands due to multiple interference orders. The TTFFGS scanned through three OH-airglow windows at 7070 Å, 8150 Å and 9090 Å, which effectively creates several narrowband filters next to each other in each window. For Hα these intervals correspond to $z \sim 0.08$, 0.24 and 0.4, respectively. A total of 13 fields have been observed, each with a diameter of $9'$, giving a total of ~ 825 sq. arcmin. Forty percent of these fields have been targetted for spectroscopic follow-up with FORS2 on the VLT. These data are currently being processed.
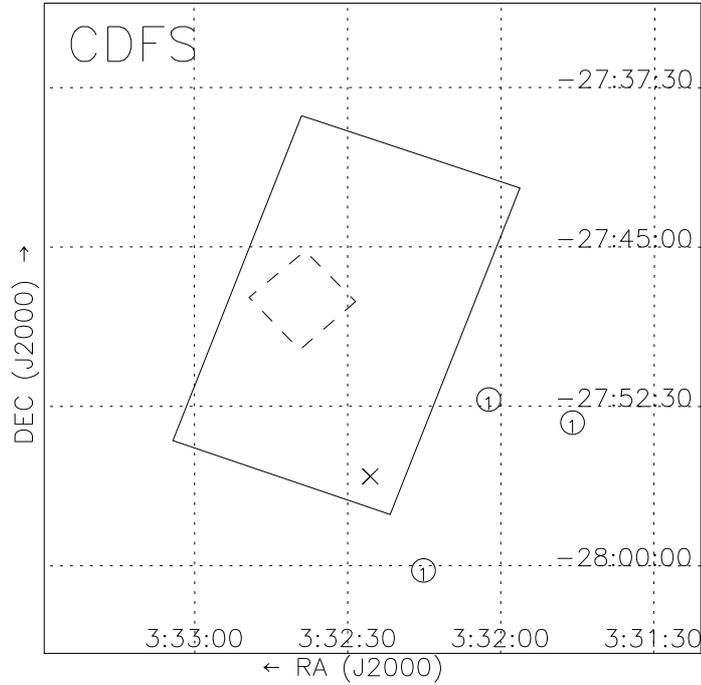
Figure 4: Sky distribution of candidate line emitters in the CDFS with North up and East to the left. The designations '1', '2' and '3' correspond to N_{810}, N_{817} and N_{824} detected candidates, respectively. The gridlines are separated by $7.'5$. In this field the Hubble Ultra Deep Field (HUDF; *dashed*) and GOODS-S (*solid*) are also shown, together with the confirmed i-drop galaxy at $z = 5.78$ of [3] (*cross*). In the CDFS there seems to be an overdensity of candidates towards the southern part of the field, similar to [11] and recent results from the HUDF [9]. No candidates were detected in the N_{817} and N_{824} filter.

References

[1] Ahn S., Lee H., Lee H. M., 2003, MNRAS, 340, 863

[2] Ajiki M., Taniguchi Y., Fujita S. S., et al., 2003, AJ, 126, 2091

[3] Bunker A. J., Stanway E. R., Ellis R. S., et al., 2003, MNRAS, 342, L47

[4] Dawson S., Spinrad H., Stern D., et al., 2002, ApJ570, 92

[5] Fujita S. S., Ajiki M., Shioya Y., et al., 2003, ApJ, 586, L115

[6] Hu E. M., Cowie L. L., Capak P, et al., 2004, AJ, 127, 563

[7] Jones D. H., Bland-Hawthorn J., 2001, ApJ, 550, 593

[8] Kewley L. J., Geller M. J., Jansen R. A, 2004, AJ, 127, 2002

[9] Malhotra S., Rhoads J. E., Pirzkal N., 2005, ApJ, 626, 666

[10] Stern D., Bunker A., Spinrad H., et al., 2000, ApJ, 537, 73

[11] Wang J. X., Malhotra S., Rhoads J. E, 2005, ApJ, 622, L77

[12] Westra E., Jones D. H., Lidman C. E., et al., 2005, A&A, 430, L21

[13] Wolf C., Meisenheimer K., Rix H.-W., 2003, A&A, 401, 73